



Infiltrated $\text{Sr}_2\text{Fe}_{1.5}\text{Mo}_{0.5}\text{O}_6/\text{La}_{0.9}\text{Sr}_{0.1}\text{Ga}_{0.8}\text{Mg}_{0.2}\text{O}_3$ electrodes towards high performance symmetrical solid oxide fuel cells fabricated by an ultra-fast and time-saving procedure



Juan Liu ^{a,b}, Yu Lei ^d, Yumei Li ^c, Jun Gao ^{a,b}, Da Han ^{d,*}, Weiting Zhan ^a, Fuqiang Huang ^a, Shaorong Wang ^{a,e,**}

^a CAS Key Laboratory of Materials for Energy Conversion, Shanghai Institute of Ceramics, Chinese Academy of Sciences (SICCAS), 1295 Dingxi Road, Shanghai 200050, PR China

^b University of the Chinese Academy of Sciences, Beijing 100049, PR China

^c Research and Test Center of Materials, Wuhan University of Technology, Wuhan 430070, PR China

^d Engineering Laboratory for Next Generation Power and Energy Storage Batteries, Graduate School at Shenzhen, Tsinghua University, Shenzhen 518055, PR China

^e China University of Mining & Technology, Jiangsu 221116, PR China

ARTICLE INFO

Article history:

Received 26 January 2017

Received in revised form 24 February 2017

Accepted 24 February 2017

Available online 27 February 2017

Keywords:

$\text{Sr}_2\text{Fe}_{1.5}\text{Mo}_{0.5}\text{O}_6$

LSGM skeleton

Ultra-fast

Symmetrical electrode

ABSTRACT

Herein, the $\text{Sr}_2\text{Fe}_{1.5}\text{Mo}_{0.5}\text{O}_6$ (SFM) precursor solution is infiltrated into a tri-layered “porous $\text{La}_{0.9}\text{Sr}_{0.1}\text{Ga}_{0.8}\text{Mg}_{0.2}\text{O}_3$ (LSGM)/dense LSGM/porous LSGM” skeleton to form both SFM/LSGM symmetrical fuel cells and functional fuel cells by adopting an ultra-fast and time-saving procedure. The heating/cooling rate when fabricating is fixed at 200 °C/min. Thanks to the unique cell structure with high thermal shock resistance and matched thermal expansion coefficients (TEC) between SFM and LSGM, no SFM/LSGM interfacial detachment is detected. The polarization resistances (R_p) of SFM/LSGM composite cathode and anode at 650 °C are 0.27 $\Omega \cdot \text{cm}^2$ and 0.235 $\Omega \cdot \text{cm}^2$, respectively. These values are even smaller than those of the cells fabricated with traditional method. From scanning electron microscope (SEM), a more homogenous distribution of SFM is identified in the ultra-fast fabricated SFM/LSGM composite, therefore leading to the enhanced performance. This study also strengthens the evidence that SFM can be used as high performance symmetrical electrode material both running in H_2 and CH_4 . When using H_2 as fuel, the maximum power density of “SFM-LSGM/LSGM/LSGM-SFM” functional fuel cell at 700 °C is 880 mW cm^{-2} . By using CH_4 as fuel, the maximum power densities at 850 and 900 °C are 146 and 306 mW cm^{-2} , respectively.

© 2017 Published by Elsevier B.V.

1. Introduction

Solid oxide fuel cell (SOFC) is one of most efficient power generation system that can convert chemical energy directly into electricity [1–4]. However, the high price and poor stability caused by its high operating temperature largely hinder its application. Reducing the operating temperature from 800 to 1000 °C to 500–700 °C is therefore highly motivated [5,6]. Consequently, development of electrodes which operated at low temperature is of great importance [7–9].

Infiltrated electrodes are widely recognized to show excellent performance even in the low temperature range [10–12]. A typical fabrication process (anode or cathode) is as follows: firstly, the precursor

solution of catalyst is infiltrated into the porous ion-conductive skeleton; then, the crystallization of catalyst is achieved by high temperature calcination at 700–900 °C for 2–4 h. One infiltration/calcination cycle normally yields a catalyst loading of 1–5 wt%. Multiply infiltration/calcination cycles are needed to increase the optimal loading to 20–40 wt% [13–15]. As indicated, such a fabrication process is time-consuming, which can hardly be adopted for large-scale application.

In our prior research, an integrated tri-layer structure of “porous LSGM/dense LSGM/porous LSGM” skeleton using for infiltrating was invented [14–16]. Impressively, we found that the quick quenching (with heating/cooling rates of 10 °C/min) has no detrimental influence on the microstructure of the infiltrated electrode when the TEC between the electrode catalyst and the LSGM skeleton are similar [15]. For further decreasing the fabrication time and increasing efficiency, the feasibility of ultra-fast fabrication of infiltrated SFM/LSGM electrode directly used for symmetrical solid oxide fuel cell is evaluated in this study. The heating/cooling rate is 200 °C/min. The preparation time of one infiltration/calcination cycle consumed is about 10 min in this study. Symmetrical solid oxide fuel cells are receiving great attention recently [17–19]. In recent years, SFM was found to be an alternative new electrode

* Corresponding author.

** Correspondence to: S. Wang, CAS Key Laboratory of Materials for Energy Conversion, Shanghai Institute of Ceramics, Chinese Academy of Sciences (SICCAS), 1295 Dingxi Road, Shanghai 200050, PR China.

E-mail addresses: handas567@sz.tsinghua.edu.cn (D. Han), srwang@cumt.edu.cn (S. Wang).

material for symmetric SOFCs showing excellent performances and also has similar TEC with LSGM [20,21]. It is therefore interesting and meaningful to investigate the performances of symmetrical fuel cells using SFM as electrode material in this study.

2. Experimental

The tri-layer structured “porous LSGM/dense LSGM/porous LSGM” skeleton was fabricated by a traditional “tape-casting/laminating/co-firing” technique [14–16]. All chemical agents were purchased from Sinopharm Chemical Reagent Co., Ltd. (China), and analytical reagents were used in this study. The SFM precursor solution was prepared by dissolving $(\text{NH}_4)_6\text{Mo}_7\text{O}_{24}\cdot 4\text{H}_2\text{O}$ (0.28 g), $\text{Sr}(\text{NO}_3)_2$ (1.32 g) and $\text{Fe}(\text{NO}_3)_2\cdot 9\text{H}_2\text{O}$ (1.89 g) in an citric acid (CA: 3.65 g) solution (30 ml) with a molar ratio between $\text{M}^{\text{n}+}$ and CA of 1:2 ($\text{M}^{\text{n}+}$ is the total concentration of metal ions). Then, ammonia solution (10 ml) containing

Ethylene Diamine Tetraacetic Acid (EDTA: 4.8 g) was added until a molar ratio between EDTA and metal ions of 1:1 was reached. The precursor solution was finally heating on a hot plate until a molar concentration of 0.2 mol L^{-1} was obtained.

A vertical tube furnace was used for heating. The temperature of the furnace was set at $850 \text{ }^\circ\text{C}$. The “porous LSGM/dense LSGM/porous LSGM” skeleton was dipped into the above SFM precursor solution for 1 min and then was drawn out. With the aid of a stainless steel hook, the skeleton with infiltrate was quickly pulled into the furnace for calcination and then was quickly fetched out of the furnace for cooling. The heating/cooling rate adopted here is $200 \text{ }^\circ\text{C}/\text{min}$, which is 20 times faster than those reported in literature [22–24]. The LSGM skeleton infiltrated with catalyst was weighed before and after each impregnation/calcination cycle to estimate the loading of the impregnated SFM. One infiltration/calcination cycle yielded an average SFM loading of 1 wt%. The infiltration/calcination process was repeated for 20 times to yield

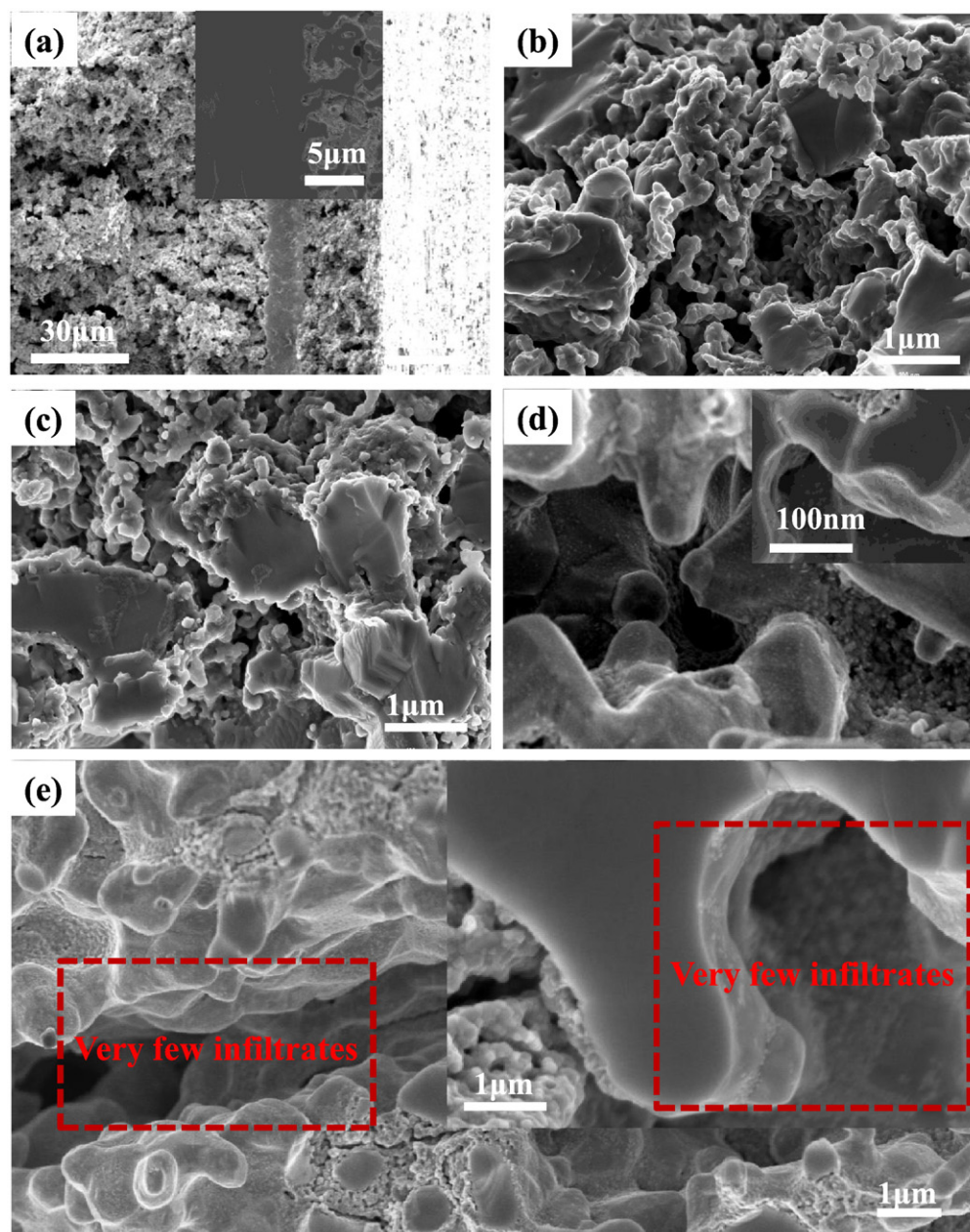


Fig. 1. (a–e) SEM image of the blank porous LSGM/dense LSGM/porous LSGM skeleton used for functional fuel cells and conductivities of SFM (a); SEM image of the SFM/LSGM cathode (b); SEM image of the SFM/LSGM anode (c); SEM image of SFM/LSGM cathode fabricated with traditional method (d,e).

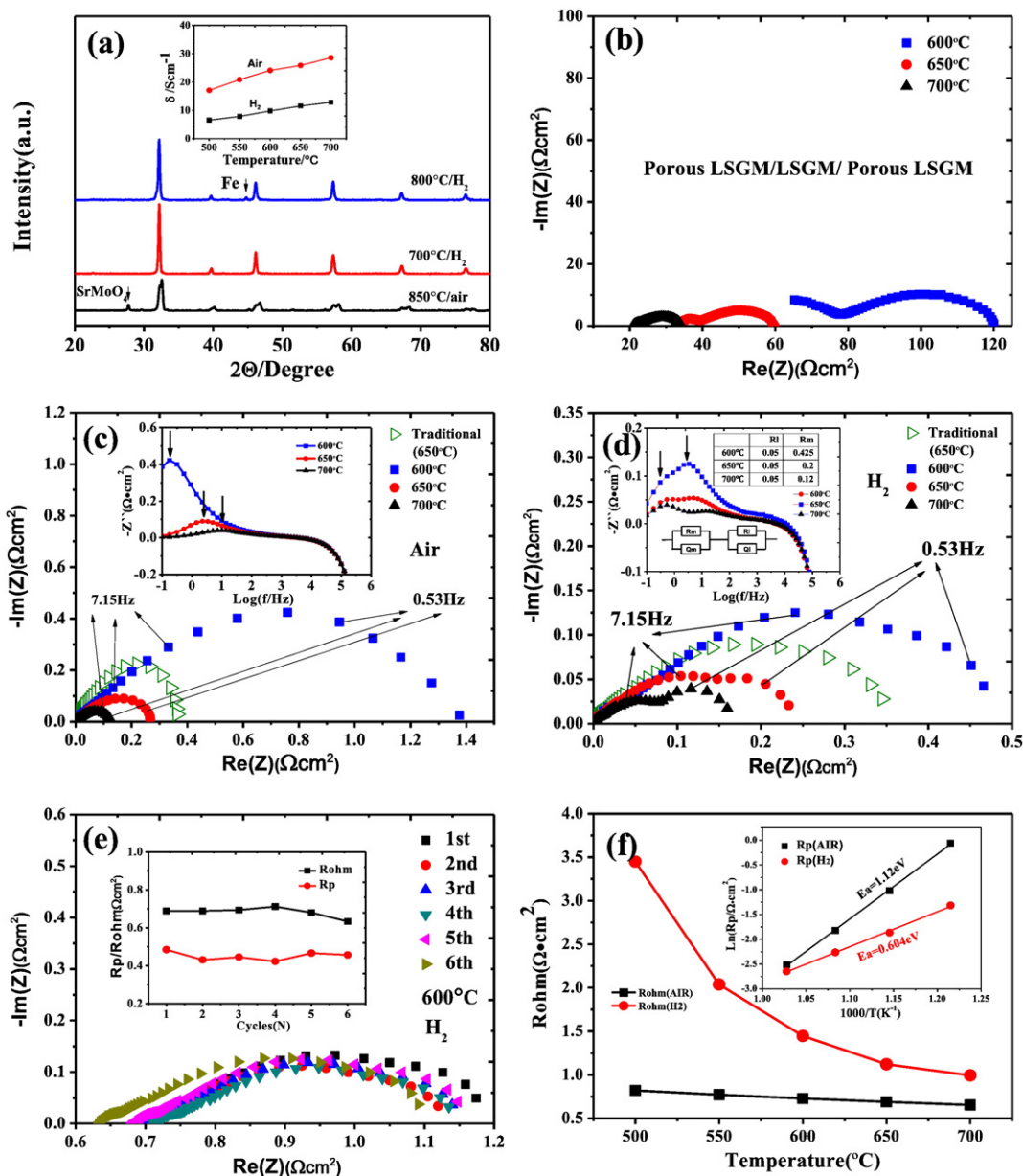


Fig. 2. (a–f) XRD patterns of the SFM powders calcined at 850 °C for 2 h and treated in H₂ atmosphere at different temperatures; conductivities of SFM in air and H₂ atmospheres (a); impedance measurements of the blank “porous LSGM/dense LSGM/porous LSGM” symmetrical fuel cell (b); EIS of the SFM/LSGM cathodes (c) and anodes (d) at temperatures of 600–700 °C; EIS of the SFM/LSGM anodes during six redox cycles at 600 °C (e); comparison of ohmic resistances of symmetrical cathode and anode fuel cells at different temperatures (f).

a final loading of 21 wt%. Prior to the testing, the holding time at 850 °C for 2 h in muffle furnace is needed for achieving crystallization of SFM. As indicated, the whole process is highly automated and can be easily adopted for large-scale application.

The microstructure of SFM/LSGM composite electrode was examined by the field emission scanning electron microscope (FESEM-4800). For electrochemical characterization, silver mesh was applied on the electrode surface using silver paste as binder for current collecting and silver wires were used as the voltage and current leads. Impedance measurement of the symmetrical fuel cells was performed in static air (or hydrogen) with an IM6 Electrochemical Workstation (ZAHNER, Germany) with a frequency ranged from 0.1 Hz to 100 kHz with amplitude of 20 mV. As for symmetrical fuel cells investigated here, the effective surface area is 0.785 cm². When testing, static air and high purity H₂ (99.999%) with flowing rate of 40 sccm were used as oxidant and fuel, respectively.

3. Result and discussion

Fig. 1a shows the SEM image of the blank “porous LSGM/dense LSGM/porous LSGM” skeleton used for single cells. The thicknesses of cathode, anode and electrolyte are 300, 25 and 18 μm, respectively. From the embedded image in Fig. 1a, we can also find that the LSGM electrolyte prepared in this study is dense. SEM images in Fig. 1b,c provide insights into the morphologies of both SFM/LSGM composite cathode (Fig. 1b) and SFM/LSGM composite anode (Fig. 1c). Nanometer sized SFM particles are uniformly coated on the LSGM skeleton. Most probably, the tri-layer structured “porous/dense/porous” skeleton used for infiltrating is outstanding for high resistance to thermal shock. No SFM/LSGM interfacial detachment is detected in this study. Furthermore, the morphologies of SFM in both air and hydrogen atmosphere revealed in Fig. 1b,c are almost identical, verifying that SFM is stable in both air and hydrogen [20]. For comparison, the SEM images

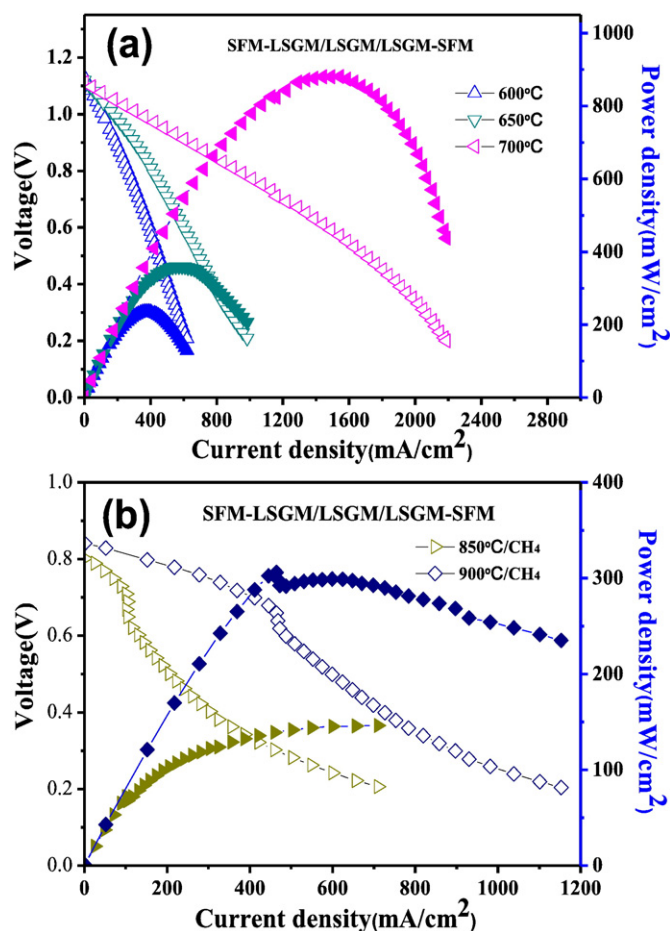


Fig. 3. (a,b) Cell voltages and power densities versus current densities of “SFM-LSGM/LSGM/LSGM-SFM” single cell at different temperatures (a: H₂; b: CH₄).

of SFM/LSGM composite electrode fabricated with traditional infiltration/calcination procedure are also shown in Fig. 1d,e. However, LSGM skeleton coated with inhomogeneous infiltrate can be easily visualized. When using the traditional fabrication method, condensation of SFM precursor solution in the skeleton was occurring as the firing temperature increasing. Owing to the none-uniform pore structure of LSGM skeleton mainly caused by poor fabrication technique which can hardly be controlled in the experiment, part of pores (mainly large pores, as indicated in Fig. 1e) in the LSGM skeleton with weak capillary force cannot be soaked with SFM precursor solution in the final stage of condensation, therefore leading to an inhomogeneous distribution of infiltrate in the skeleton. On the contrary, when firing very quickly, the SFM precursor solution burned out instantly, thus insuring a much more homogenous distribution of infiltrate.

From XRD patterns indicated in Fig. 2a, SFM emerges as the main phase. A little amount of SrMoO₄ can also be detected. When reduced at high temperature, SrMoO₄ is transferred to perovskite-type oxide SrMoO₃. Mainly owing to the similar XRD characteristic peaks between SrMoO₃ and SFM, SrMoO₃ is not visible in the XRD patterns. As indicated, when operating at low temperature in reduced atmosphere, SFM is considered to be stable. Compared with the widely used Co-based electrode materials, the conductivities of SFM (density: 98%) are much lower, which showed in Fig. 2a. Impedance measurements of the “porous LSGM/dense LSGM/porous LSGM” symmetrical fuel cell are presented in Fig. 2b, showing very large Rohm. However, when using SFM as catalyst which preserving low conductivity, much lower Rp of both the SFM/LSGM cathode and anode in the temperature range of 600–

700 °C are shown in Fig. 2c,d. Analyzing from Nyquist and Bode plots in Fig. 2c,d, the oxygen-exchange reaction and charge transfer reaction on SFM surfaces dominates the cathode and anode kinetics, respectively [25,26].

The Rp of both cathode and anode at 650 °C (0.27 Ω·cm² and 0.235 Ω·cm², respectively) fabricated by our modified procedure are smaller than those fabricated by traditional method. This finding is enlightening. As for the real application, fuel cells with large size are urgently required. The inhomogeneous distribution of infiltrate in the fuel cells with large size may lead to ugly performance. The research in this study probably provides a solution. Fig. 2e compares the Electrochemical Impedance Spectroscopy (EIS) of symmetrical fuel cells in H₂ atmosphere at 600 °C during six redox cycles. Prior to the redox cycling, the Rohm and Rp of the SFM/LSGM composite anode are 0.715 Ω·cm² and 0.46 Ω·cm². After 6 redox cycles, the Rohm and Rp are 0.63 Ω·cm² and 0.42 Ω·cm², indicating fairly stable performances. The Rohm of symmetrical cathode and anode fuel cells at 600 °C are as large as 0.727 Ω·cm² and 1.414 Ω·cm² (electrolyte thickness: 40 μm), as revealed in Fig. 2f. We can expect that the Rohm can be reduced by decreasing the thickness of electrodes, using new electrode material with high conductivity or increasing SFM loading (21 wt% is not the optimal loading) [27]. Fig. 2f further compares the Rohm of such symmetrical electrode fuel cells. The Rohm of cathode in the temperature range investigated are much smaller than those of the anode. This is reasonable because the conductivity of SFM in air is much higher than that in hydrogen atmosphere. Also shown in Fig. 3f are the catalytic activities of SFM towards oxygen reduction and hydrogen oxidation. The SFM/LSGM composite anode shows a much smaller Rp with lower activation energy.

Plots of cell voltages and power densities versus current densities of the symmetrical functional fuel cell are shown in Fig. 3a. When using H₂ as fuel and air as oxidant, the maximum power densities recorded are 880, 359 and 236 mW cm⁻² at 700, 650 and 600 °C, respectively. The performances of single cells investigated here are higher than those of the previously reported symmetrical SOFCs. For example, when using La_{0.6}Sr_{0.4}Fe_{0.9}Sc_{0.1}O₃, PrBa_{0.8}Ca_{0.2}Mn₂O₅ and La_{0.9}Ca_{0.1}Fe_{0.9}Nb_{0.1}O₃ as electrodes, the maximum power densities are only 320, 502 and 204 mW cm⁻² at 700 °C, respectively [26,28,29]. The performance of the symmetrical functional fuel cell when operated in CH₄ (3% H₂O) is also shown in Fig. 3b. The open circuit voltages (OCV) at 850 °C and 900 °C are 0.9 V and 0.75 V, while the maximum power densities are 146 and 306 mW cm⁻² respectively. The low OCV indicates that the catalytic property of SFM for methane oxidation is still limited. Similar low OCV values can also be found in fuel cells when using SFM, La_{0.75}Sr_{0.25}Cr_{0.5}Mn_{0.5}O₃ and Sr₂FeNb_{0.2}Mo_{0.8}O₆ as anodes [30–32]. The sudden change of CV curves at 0.7 V is most probably attributed to a special activation process or the structural instability of SFM at high temperature.

Notably, the fuel cells investigated have small diameters of 1 cm. The feasibility of fast preparation of large cells at such fast heating/cooling rates is under investigation now. Furthermore, the fast preparation of electrolyte and metal supported fuel cells with high mechanical strength is also under consideration.

4. Conclusion

The feasibility of fast preparation of SFM/LSGM composite electrode has been carefully evaluated in this study. No interfacial detachment is found between SFM and the LSGM skeleton. Both the SFM/LSGM composite cathode and composite anode fabricated with this method showed robust and extraordinary electrochemical performances. The maximum power densities of single cell when using H₂ as fuel are as high as 880, 359 and 236 mW cm⁻² at 700, 650 and 600 °C, respectively. When using CH₄ as fuel, the maximum power densities are 146 and 306 mW cm⁻² at 850 °C and 900 °C, respectively.

Acknowledgement

This work was supported by Shenzhen Basic Research Program (JCYJ20150331151536444). Thanks for careful discussion and FE-SEM testing provided by Research and Test Center of Materials, Wuhan University of Technology.

References

- [1] N.Q. Minh, Ceramic fuel-cells, *J. Am. Ceram. Soc.* 76 (1993) 563.
- [2] R. Riedel, I.W. Chen, *Ceramic Fuel Cells: Principles, Materials, and Applications* 4 (4) (2013) 345–371.
- [3] N. Mahato, A. Banerjee, A. Gupta, S. Omar, K. Balani, Progress in material selection for solid oxide fuel cell technology: a review, *Prog. Mater. Sci.* 72 (2015) 141–337.
- [4] B.C. Steele, A. Heinzl, *Materials for fuel-cell technologies*, *Nature* 414 (6861) (2001) 345–352.
- [5] E.D. Wachsman, K.T. Lee, Lowering the temperature of solid oxide fuel cells, *Science* 334 (2011) 935–939.
- [6] Z. Shao, S.M. Haile, A high-performance cathode for the next generation of solid-oxide fuel cells, *Nature* 431 (7005) (2004) 170–173.
- [7] W. Zhou, Z. Shao, R. Ran, R. Cai, Novel $\text{SrSc}_{0.2}\text{Co}_{0.8}\text{O}_{3-\delta}$ as a cathode material for low temperature solid-oxide fuel cell, *Electrochem. Commun.* 10 (2008) 1647–1651.
- [8] S. Lü, G. Long, X. Meng, Y. Ji, B. Lü, H. Zhao, $\text{PrBa}_{0.5}\text{Sr}_{0.5}\text{Co}_2\text{O}_{5+x}$ as cathode material based on LSGM and GDC electrolyte for intermediate-temperature solid oxide fuel cells, *Int. J. Hydrog. Energy* 37 (2012) 5914–5919.
- [9] A. Tarancon, J. Penamartinez, D. Marrero-Lopez, A. Morata, J. Ruizmorales, P. Nunez, Stability, chemical compatibility and electrochemical performance of $\text{GdBaCo}_2\text{O}_{5+x}$ layered perovskite as a cathode for intermediate temperature solid oxide fuel cells, *Solid State Ionics* 179 (2008) 2372–2378.
- [10] Changrong Xia, William Rauch, Fanglin Chen, et al., $\text{Sm}_{0.5}\text{Sr}_{0.5}\text{CoO}_3$ cathodes for low-temperature SOFCs, *Solid State Ionics* 149 (2002) 11–19.
- [11] S.P. Jiang, Nanoscale and nano-structured electrodes of solid oxide fuel cells by infiltration: advances and challenges, *Int. J. Hydrog. Energy* 37 (2012) 449–470.
- [12] J.M. Vohs, R.J. Gorte, High-performance SOFC cathodes prepared by infiltration, *Adv. Mater.* 21 (2009) 943–956.
- [13] X. Li, N. Xu, X. Zhao, K. Huang, Performance of a commercial cathode-supported solid oxide fuel cells prepared by single-step infiltration of an ion-conducting electrocatalyst, *J. Power Sources* 199 (2012) 132–137.
- [14] D. Han, H. Wu, J. Li, S. Wang, Z. Zhan, Nanostructuring of $\text{SmBa}_{0.5}\text{Sr}_{0.5}\text{Co}_2\text{O}_{5+\delta}$ cathodes for reduced-temperature solid oxide fuel cells, *J. Power Sources* 246 (2014) 409–416.
- [15] D. Han, Y. Liu, S. Wang, Z. Zhan, Co-infiltrating $\text{Pr}_{0.6}\text{Sr}_{0.4}\text{FeO}_3\text{-Ce}_{1-x}\text{Pr}_x\text{O}_2$ ($x = 0.1, 0.3, 0.5, 0.7, 0.9$) mixed oxides into the $\text{La}_{0.9}\text{Sr}_{0.1}\text{Ga}_{0.8}\text{Mg}_{0.2}\text{O}_3$ skeleton for use as low temperature solid oxide fuel cell cathodes, *Electrochim. Acta* 143 (2014) 168–174.
- [16] D. Han, Y. Liu, S. Wang, Z. Zhan, Enhanced performance of solid oxide fuel cell fabricated by a replica technique combined with infiltrating process, *Int. J. Hydrog. Energy* 39 (2014) 13217–13223.
- [17] S. Tao, J.T. Irvine, A redox-stable efficient anode for solid-oxide fuel cell, *Nat. Mater.* 2 (5) (2003) 320–323.
- [18] J.C. Ruiz-Morales, J. Canales-Vázquez, B. Ballesteros-Pérez, J. Peña-Martínez, D. Marrero-López, J.T.S. Irvine, P. Núñez, LSCM-(YSZ-CGO) composites as improved symmetrical electrodes for solid oxide fuel cells, *J. Eur. Ceram. Soc.* 27 (2007) 4223–4227.
- [19] D.M. Bastidas, S. Tao, J.T.S. Irvine, A symmetrical solid oxide fuel cell demonstrating redox stable perovskite electrodes, *J. Mater. Chem.* 16 (2006) 1603–1605.
- [20] Qiang Liu, Xihui Dong, Guoliang Xiao, Fei Zhao, Fanglin Chen, A novel electrode material for symmetrical SOFCs, *Adv. Mater.* 22 (2010) 5478–5482.
- [21] A.J. Fernández-Ropero, J.M. Porras-Vázquez, A. Cabeza, P.R. Slater, D. Marrero-López, E.R. Losilla, High valence transition metal doped strontium ferrites for electrode materials in symmetrical SOFCs, *J. Power Sources* 249 (2014) 405–413.
- [22] Burye Theodore E., Jason D. Nicholas, Precursor solution additives improve desiccated $\text{La}_{0.6}\text{Sr}_{0.4}\text{Co}_{0.8}\text{Fe}_{0.2}\text{O}_3$ infiltrated solid oxide fuel cell cathode performance, *J. Power Sources* 301 (2016) 287–298.
- [23] Jiangwei Ju, Jie Lin, Yusu Wang, Yanxiang Zhang, Changrong Xia, Electrical performance of nanostructured strontium-doped lanthanum manganite impregnated onto yttria-stabilized zirconia backbone, *J. Power Sources* 302 (2016) 298–307.
- [24] Augusto Mejía Gómez, Joaquín Sacanell, Ana Gabriela Leyva, Diego G. Lamas, Performance of $\text{La}_{0.6}\text{Sr}_{0.4}\text{Co}_{1-y}\text{Fe}_y\text{O}_3$ ($y = 0.2, 0.5$ and 0.8) nanostructured cathodes for intermediate-temperature solid-oxide fuel cells: influence of microstructure and composition, *Ceram. Int.* 142 (2016) 3145–3155.
- [25] Da Han, Xuejiao Liu, Fanrong Zeng, Jiqin Qian, Tianzhi Wu, Zhongliang Zhan, A micro-nano porous oxide hybrid for efficient oxygen reduction in reduced-temperature solid oxide fuel cells, *Sci. Rep.* 2, 462.
- [26] X. Liu, D. Han, Y. Zhou, X. Meng, H. Wu, J. Li, F. Zeng, Z. Zhan, Sc-substituted $\text{La}_{0.6}\text{Sr}_{0.4}\text{FeO}_{3-\delta}$ mixed conducting oxides as promising electrodes for symmetrical solid oxide fuel cells, *J. Power Sources* 246 (2014) 457–463.
- [27] R. Lan, P.I. Cowin, S. Sengodan, S. Tao, A perovskite oxide with high conductivities in both air and reducing atmosphere for use as electrode for solid oxide fuel cells, *Sci. Report.* 6 (2016) 31839.
- [28] S. Choi, S. Sengodan, S. Park, Y.W. Ju, J. Kim, J. Hyodo, H.Y. Jeong, T. Ishihara, J. Shin, G. Kim, A robust symmetrical electrode with layered perovskite structure for direct hydrocarbon solid oxide fuel cells: $\text{PrBa}_{0.8}\text{Ca}_{0.2}\text{Mn}_2\text{O}_{5+\delta}$, *J. Mater. Chem. A* 4 (2016) 1747–1753.
- [29] X. Kong, X. Zhou, Y. Tian, X. Wu, J. Zhang, W. Zuo, Niobium doped lanthanum calcium ferrite perovskite as a novel electrode material for symmetrical solid oxide fuel cells, *J. Power Sources* 326 (2016) 35–42.
- [30] Z. Wang, Y. Tian, Y. Li, Direct CH_4 fuel cell using $\text{Sr}_2\text{FeMoO}_6$ as an anode material, *J. Power Sources* 196 (2011) 6104–6109.
- [31] S. Jiang, X. Chen, S. Chan, J. Kwok, K. Khor, $(\text{La}_{0.75}\text{Sr}_{0.25})(\text{Cr}_{0.5}\text{Mn}_{0.5})\text{O}_3/\text{YSZ}$ composite anodes for methane oxidation reaction in solid oxide fuel cells, *Solid State Ionics* 177 (2006) 149–157.
- [32] H. Ding, Z. Tao, S. Liu, Y. Yang, A redox-stable direct-methane solid oxide fuel cell (SOFC) with $\text{Sr}_2\text{FeNb}_{0.2}\text{Mo}_{0.8}\text{O}_{6-\delta}$ double perovskite as anode material, *J. Power Sources* 327 (2016) 573–579.